

approaches are used, based on the formation of the metal NPs in the DNA-NP conjugate. In this research, the *ex situ* method was employed because the researchers discovered that negatively charged THP-AuNPs can bind densely to the negatively charged calf thymus DNA. During the metallization procedure, DNA was first immobilized on a silicon substrate by O<sub>2</sub> plasma treatment to enhance immobilization and spin-coating to elongate the molecules. Before the THP-AuNP sol was applied to the substrate, the particles were precipitated in ethanol, then dissolved in an ethanol-water solution. Optimum results with respect to density of particle templating, avoidance of excess particles on the substrate, and lack of defects in the resultant wires were obtained at an ethanol:water ratio of 95:5. After rinsing and drying, the samples were treated with an electroless gold plating solution in order to form conductive nanowires for further characterization.

Atomic force microscopy revealed that after calf thymus DNA molecules on a silicon substrate were treated with THP-AuNPs in 95% ethanol, the DNA molecules were decorated with particles, with some excess particles (0.7 nm to 2 nm in size) also on the substrate. Scanning electron microscopy images showed that the electroless gold plating of the resulting DNA-AuNP conjugates provides nanowires ~30–40 nm in width and longer than 2 μm. The good contrast against the silicon surface indicates high conductivity and the metallization was restricted almost entirely to the DNA. The results of the electrical transport capabilities of the DNA nanowires showed that their electrical conductivities were about one-thousandth that of bulk gold.

To determine what kind of mechanism controls the binding between THP-AuNPs and DNA, several hypotheses were considered, based on the interactions between THP-AuNPs and DNA, such as adsorption of THP-AuNPs to hydrophilic DNA molecules on the silicon oxide surface, hydrogen-bonding interactions in between, ligand replacement by groups on DNA that can coordinate to the AuNP surface, and the covalent bonding between THP and amino groups of the DNA base.

The process can be finished in ~10 min, but the *in situ* approaches that employ metal salts or complexes as precursors take longer than 1 h. The technique reported here by O. Harnack and co-workers could be used for future electronic circuits because it can lower the fabrication cost and is suitable for feature sizes below the current limit of optical lithography. However, issues about the binding mechanism between the

THP-AuNPs and DNA, and how the solvent and substrate influence the process, need to be further studied.

YUE HU

### Direct Ink-Jet Printing Assembles ZrO<sub>2</sub> Powder into 3D Shape

Three-dimensional shapes can be created from ceramic powders by forcing droplets of “ink” containing the powder through an ink-jet nozzle, layering the deposition to generate height. Xinglong Zhao and colleagues from the University of London in conjunction with Jin-Hua Song from Brunel University report their work on the creation of vertical walls from ceramic materials using ink-jet printing in the August issue of the *Journal of the American Ceramic Society*. Zhao and colleagues have created mazes (replicas of one at Hampton Court Palace outside London) with various wall-thickness values where the smallest gap between walls was  $170 \pm 10 \mu\text{m}$ . This technique has applications in rapid prototyping and the creation of ceramic molds, circuit boards, and biosensors.

A ZrO<sub>2</sub> powder with an average particle size of 0.45 μm was mixed with a commercial dispersant to create a mixture with an estimated ZrO<sub>2</sub> powder volume fraction of 0.63. The combination was then stirred with an ultrasonic probe for 5 min and milled for approximately 30 min to disperse the powder into the liquid and break down the agglomerates. The ink-jet print head contained 500 50-μm nozzles with a print width of 70 mm and a computer-controlled sliding table. The table print speed was 500 mm/s and registered its position at the edge of the track between passes to ensure accuracy in the *y* printing direction. To assure uniformity, the ink was filtered through a 5-μm mesh, and the air was removed from the system by repeated extraction and insertion of the ink through the print head until no signs

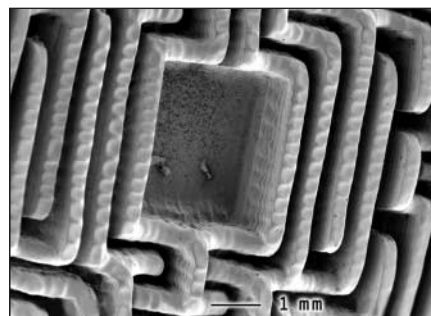


Figure. Scanning electron micrograph of vertical ceramic walls created by direct ceramic ink-jet printing.

of bubbles appeared in the tubing. Between passes, a hot-air blower was used for 20 s to enhance the drying procedure and reduce spreading. Since the ink remained opaque after 10 h, the final samples were allowed to dry for 24 h before pyrolyzation and sintering.

The results of this process based on a maze pattern can be seen in the figure. Although individual droplets cannot be seen, an overall surface texture results in part from coalescence during the drying process. Very straight vertical walls were achieved, although the height was not uniform due to a wall-thickness effect, where thinner walls had reduced height, and also because of in-filling of the center parts of the maze. The researchers said that complications resulting from ink drying and spreading will need to be considered during the scaling-up process.

CHRISTINE RUSSELL

### Simulations Show a Hexatic Phase in Porous Media

In the Kosterlitz–Thouless–Halperin–Nelson–Young (KTHNY) theory, when a two-dimensional crystal melts, it first becomes hexatic by the unbinding of dislocation pairs, and then becomes liquid through the unbinding of disclination pairs. However, early simulations did not exhibit the hexatic phase. Now, researchers at the Massachusetts Institute of Technology, North Carolina State University, and Adam Mickiewicz University in Poland have observed the hexatic phase, consistent with the theory, in molecular simulations of simple fluids in narrow slit-shaped carbon pores. The stability of the phase increased with the strength of the fluid–wall interaction. Experimental measurements confirmed the existence of the hexatic phase.

In Monte Carlo simulations of large systems of the order of 64,000 molecules, the crystalline–hexatic and hexatic–liquid transitions were observed for simple fluids of spherical molecules. R. Radhakrishnan of MIT and co-workers reported in the August 12 issue of *Physical Review Letters* that they modeled the fluid–fluid interaction of CCl<sub>4</sub> with a Lennard–Jones potential and the fluid–wall interaction with a 10-4-3 Steele potential.

The simulated pores were of two different widths, 0.911 nm or 1.41 nm, and contained either one or two layers of adsorbed CCl<sub>4</sub>. The researchers monitored the in-plane positional and orientational correlation functions to determine the nature of the confined phase.

For the two-layer system, at 360 K the positional correlation function was isotropic, and the orientational one showed

exponential decay, representing a liquid phase. At 330 K, the positional correlation function remained isotropic but the orientational one showed algebraic decay, a signature of the hexatic phase. At 290 K, the system became a two-dimensional hexagonal crystal, showing quasi-long-range positional order and long-range orientational order. The scaling of the correlation functions was consistent with KTHNY theory.

The melting transition was second order when the pores contained one layer of molecules and became weakly first order for pores containing two layers. The researchers attribute the change to interaction between defect configurations in the two layers.

Differential scanning calorimetry (DSC) measurements of  $\text{CCl}_4$  and aniline in an activated carbon fiber with slit-shaped pores narrowly distributed around a mean size of 1.4 nm showed peaks near temperatures predicted in the simulations. Nonlinear dielectric effect (NDE) signals diverged with a scaling consistent with the theory.

Dielectric relaxation spectroscopy (DRS) of adsorbed aniline, a dipolar fluid, showed sharp changes, indicating phase transitions near the predicted temperatures. The orientational relaxation times of the adsorbed molecules were typical of a hexatic phase between 298 K and 324 K. Below that range, the time scales were typical of a crystal, and above it, they were typical of a liquid.

ELIZABETH A. SHACK

### Direct Observation of Intercalated Cs in Zeolite $\text{Si}_{32}\text{O}_{64}$ Yields Example of Inorganic Electride

Understanding the properties of nanoscale arrays of metal atoms may allow scientists to manipulate these properties to produce nanomagnets, nanocatalysts, nanodevices, and composites with better optical properties than are currently possible. However, such applications require a detailed knowledge of the materials' atomic-level structure. Thomas Vogt, a physicist at Brookhaven National Laboratory, and scientists from Michigan State University led by physicist Valeri Petkov (now at Central Michigan University), have demonstrated that the atomic pair distribution function (PDF) technique allows them to decipher such fine-level nanostructures.

Their analysis of a material composed of cesium ions trapped inside nano-sized pores of the silicon oxide zeolite  $\text{Si}_{32}\text{O}_{64}$  is described in the August 12 issue of *Physical Review Letters*. This material is also the first example of a room-temperature inorganic "electride," a stable separation

of positively charged cations and electrons with properties determined by the topology of the pores in the host matrix.

In traditional crystallography, long-range order and symmetry, specifically the repeating three-dimensional (3D) patterns in the crystals, give rise to sharp Bragg peaks in the x-ray powder diffraction pattern, which are then used to determine the atomic structures. Materials constructed at the nanoscale, however, lack this long-range order and often accommodate a large number of defects and local disorder. The result, said Petkov, is that the diffraction patterns of nanocrystals are much more diffuse with few, if any, Bragg peaks.

To overcome this problem, the team of scientists employed the PDF technique, a nontraditional experimental approach, to read between the Bragg peaks of data produced by traditional x-ray powder diffraction experiments. With the PDF technique, the scientists revealed direct structural evidence that cesium is intercalated in the nano-sized pores of the silicon oxide zeolite in the form of positively charged cesium ions arranged in short-range-order

zigzag chains. This verifies that  $\text{Cs}_x\text{Si}_{32}\text{O}_{64}$  is a room-temperature stable inorganic electride, the scientists said.

"Electrides are novel materials that are just beginning to be studied," said Petkov. First results show that they could be used as reducing materials in chemical synthesis of other materials and that they have useful electronic properties such as low-energy electron emission.

### Carbon-Nanotube Transistor Arrays Used for Fabrication of Multistage Complementary Logic Devices and Ring Oscillators

Carbon nanotubes are expected to be the most promising candidates for building blocks for the next generation of electronic devices, predominantly due to low surface scattering and nanoscale channel widths. A group of researchers at the Department of Chemistry and the Laboratory for Advanced Materials at Stanford University have demonstrated a fabrication route for multistage complementary NOR, OR, NAND, and AND logic gates and ring oscillators based on arrays of *p*- and *n*-type

C O O L U N D E R P R E S S U R E

## Hall Measurement System

MMR's low cost, Turnkey Hall Effect Measurement System provides user programmed computer controlled measurement and data acquisition over a temperature range of -200°C to +300°C – without the use of liquid nitrogen. The system measures magneto resistivity, four point resistivity, sheet resistivity, sheet number, mobility, Hall coefficient, and carrier density using the Van der Pauw and Hall measurement techniques.

Measurement Ranges (somewhat dependent on sample thickness)	
Resistivity	10 <sup>-4</sup> Ohm-cm to 10 <sup>+13</sup> Ohm-cm
Carrier Mobility	1cm <sup>2</sup> / volt-sec to 10 <sup>+7</sup> cm <sup>2</sup> / volt-sec
Carrier Density	10 <sup>+3</sup> cm <sup>-3</sup> to 10 <sup>+19</sup> cm <sup>-3</sup>

For more information about the Hall Effect Measurement System, contact Bob Paugh at 650 / 962-9620 or bobp@mmr.com. Or visit our web page at <http://www.mmr.com>.

MMR Technologies, Inc.

Circle No. 12 on Inside Back Cover